

THE USE OF TRANSITIONAL ELEMENTS FOR STRESS ANALYSIS OF STRUCTURES WITH A TECHNOLOGICAL SURFACE LAYER BY THE METHOD OF FINITE ELEMENTS

S. K U C H A R S K I (WARSZAWA)

Some shape functions have been presented for a transitional finite element, the use of which facilitates stress analysis of a structure with a technological surface layer. An example of application of such an element for determining the state of stress in a notched specimen with a surface layer is discussed.

1. INTRODUCTION

The influence of a technological surface layer on the strength of a machine element is confirmed by an increasing number of investigations, both theoretical and numerical. The problem of determining stresses in a technological surface layer is of a continually growing importance. A most universal tool for calculating stresses in machine parts is the finite element method. In the case of structures with a technological surface layer, application of typical finite elements which are used with the existing FEM-systems comes up against some difficulties resulting from the fact that the modelling of variation of the material properties in the very small region of the surface layer requires very fine element meshes in the zone of that layer. This makes the stress analysis laborious in the phase of design of the meshes and later, when a system of equations with, a very high number of unknowns is to be solved. To moderate those difficulties a novel type of finite element has been developed, the use of which makes the mesh refinement procedure more effective than in the case of traditional elements. This effectiveness property will be discussed in Sec. 2. The idea of accounting for the surface layer in the stress analysis by the method of finite elements is comparatively new and has been treated in [1] and [2]. Some recent examples of application of the finite element analysis can be found in [3], [4] and [5]. In [1] membrane elements are used for modelling the surface layer, which is an approximation, because the stress component normal to the layer (therefore also to the

surface of the structure) is rejected. By applying the membrane model to various layers, the authors showed that such an approximation may lead, in the case of sharp notches, to serious errors. Thus, for instance, it has been found that, in the case of sharp annular notches, the stress σ_r at the bottom of a notch (Fig. 1), immediately below the surface layer, may reach a value of a few scores of MPa.

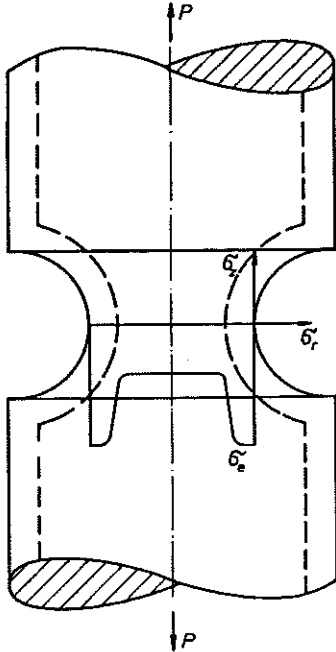


FIG. 1. Directions of stress components at the bottom of a notch and a diagram of variation of the yield point (σ_e).

From the equilibrium equations it follows that, at a point of the layer located near the core, the stress σ_r is of the same order of magnitude, while the membrane model requires the same stress component in the layer to be zero. Thus, if there are stress concentrators (sharp notches, concentrated loads), it appears to be reasonable to use traditional elements, and, at the same time, to try to moderate the difficulties mentioned above.

One of the methods for reaching that aim is to use a transitional finite element which can be combined with the traditional elements, thus making possible the effective mesh refinement. This problem is the subject matter of the present paper.

2. DESCRIPTION OF THE ELEMENT

The finite element used for plane and axially symmetric stress and strain analysis is, in many systems of finite element analysis, an isoparametric

quadrangular eight-node element. If this type of element is the only one used, mesh element can be introduced on a rather limited scale. Somewhat better results may be obtained if the same elements are used together with triangular ones. To obtain a still better effect, an element has been developed as that represented in Fig. 2.

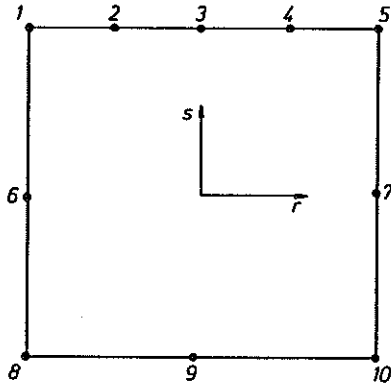


FIG. 2. The proposed element.

It is a ten-node isoparametric element, the number of nodes on one edge (5) being greater than that on each of the remaining edges (3). The location of the nodes enables us to combine the element with traditional eight-node elements, thus making the element meshes finer according to the diagram in Fig. 3a. Figure 3b shows, for comparison, element meshes made finer by introducing triangular elements. It is seen that element proposed here can replace three triangular elements.

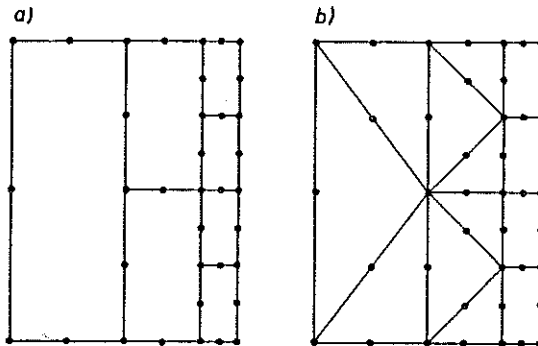


FIG. 3. Diagrammatic representation of element meshes refined by using a) elements of the proposed type and b) triangular elements.

The number of nodes on the edge 1-5 of the element being greater, the shape functions for the nodes 1 to 5, which depend on the variable r , must

constitute polynomials of higher orders than the shape functions depending on s . As a consequence, the dimension of an element in the r -direction may be greater than that in the s -direction with the same accuracy of approximation. This enables us to refine the mesh by a method illustrated in Fig. 3, which takes into consideration the fact that the dimension of the surface layer is smaller in one direction than in the remaining directions. The design of element meshes according to the scheme of Fig. 3 makes possible effective connection of a region of small elements to a region of large elements.

3. THE SHAPE FUNCTIONS OF AN ELEMENT

The shape functions of an element have been developed according to the directions given in [6]. Assuming the numbers of nodes according to Fig. 3, the shape functions can be written as follows.

$$h_1 = \frac{1}{6} \left(2r^4 - 2r^3 - \frac{1}{2}r^2 + \frac{1}{2}r \right) (1+s) - \frac{1}{4}(1-s^2)(1-r),$$

$$h_2 = \frac{4}{3}(-2r^4 + r^3 + 2r^2 - r)\frac{1}{2}(1+s),$$

$$h_3 = (4r^4 - 5r^2 + 1)\frac{1}{2}(1+s),$$

$$h_4 = \frac{4}{3}(-2r^4 - r^3 + 2r^2 + r)\frac{1}{2}(1+s),$$

$$h_5 = \frac{1}{3} \left(2r^4 + 2r^3 - \frac{1}{2}r^2 - \frac{1}{2}r \right) \frac{1}{2}(1+s) - \frac{1}{4}(1-s^2)(1+r),$$

$$h_6 = \frac{1}{2}(1-s^2)(1-r),$$

$$h_7 = \frac{1}{2}(1-s^2)(1+r),$$

$$h_8 = \frac{1}{4}(1-r)(1-s) - \frac{1}{4}(1-s^2)(1-r) - \frac{1}{4}(1-r^2)(1-s),$$

$$h_9 = \frac{1}{2}(1-r^2)(1-s),$$

$$h_{10} = \frac{1}{4}(1+r)(1-s) - \frac{1}{4}(1-r^2)(1-s) - \frac{1}{4}(1-s^2)(1+r).$$

The shape functions for the nodes 1 to 5 are shown in Fig. 4, those for the remaining nodes being the same as in the traditional eight-node elements.

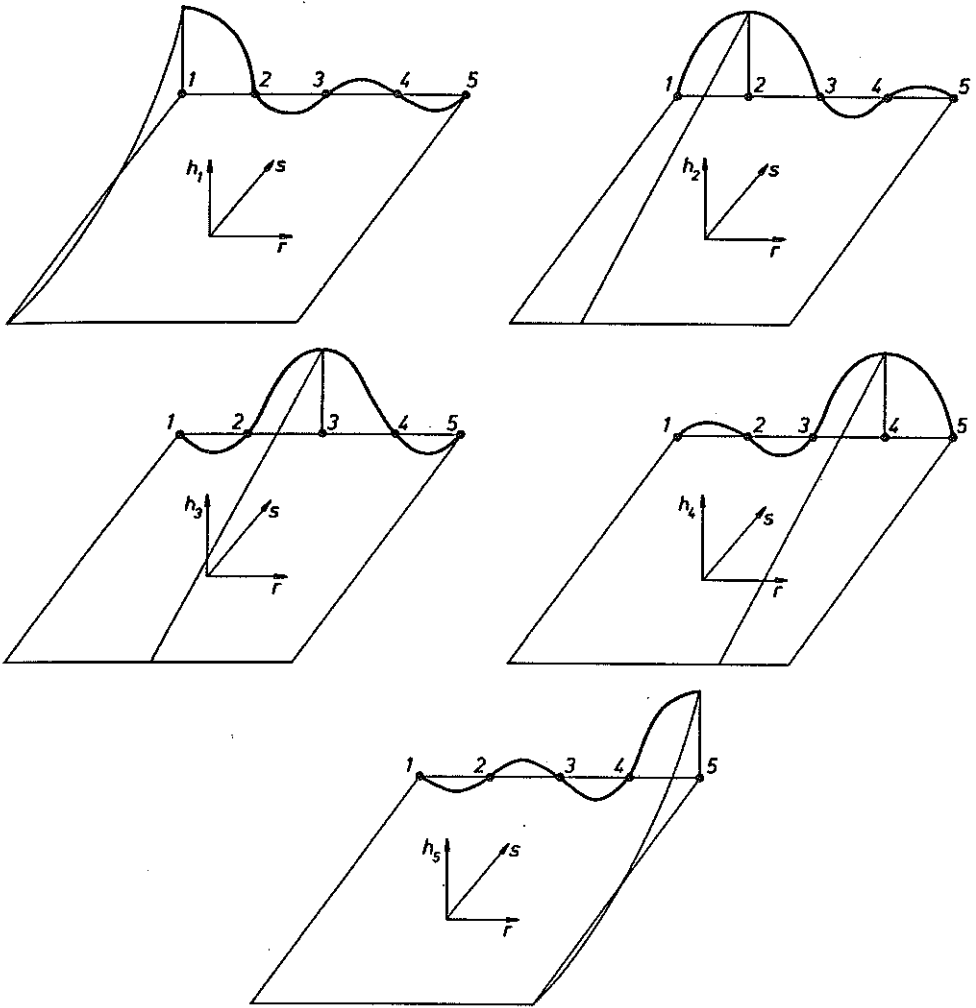


FIG. 4. Shape functions of an element (for the nodes 1 to 5).

To determine the stiffness matrix we must first determine the derivatives of the shape functions. They are as follows.

$$\frac{\partial h_1}{\partial r} = \frac{1}{6} \left(2r^3 - 6r^2(1-r) - r + \frac{1}{2} \right) (1+s) + \frac{1}{4}(1-s^2),$$

$$\frac{\partial h_1}{\partial s} = \frac{1}{6} \left(2r^4 - 2r^3 - \frac{1}{2}r^2 + \frac{1}{2}r \right) + \frac{1}{2}s(1-r),$$

$$\frac{\partial h_2}{\partial r} = \frac{4}{3}(-8r^3 + 3r^2 + 4r - 1) \cdot \frac{1}{2}(1+s),$$

$$\frac{\partial h_2}{\partial s} = \frac{4}{3} \left(-r^4 + \frac{1}{2}r^3 + r^2 - \frac{1}{2}r \right),$$

$$\frac{\partial h_3}{\partial r} = (8r^3 - 5r)(1 + s),$$

$$\frac{\partial h_3}{\partial s} = \frac{1}{2}(4r^4 - 5r^2 + 1),$$

$$\frac{\partial h_4}{\partial r} = \frac{4}{6}(-8r^3 - 3r^2 + 4r + 1)(1 + s),$$

$$\frac{\partial h_4}{\partial s} = \frac{4}{3} \left(-r^4 - \frac{1}{2}r^3 + r^2 + \frac{1}{2}r \right),$$

$$\frac{\partial h_5}{\partial r} = \frac{1}{6} \left(8r^3 + 6r^2 - r - \frac{1}{2} \right) (1 + s) - \frac{1}{4}(1 - s^2),$$

$$\frac{\partial h_5}{\partial s} = \frac{1}{6} \left(2r^4 + 2r^3 - \frac{1}{2}r^2 - \frac{1}{2}r \right) + \frac{1}{2}s(1 + r),$$

$$\frac{\partial h_6}{\partial r} = -\frac{1}{2}(1 - s^2),$$

$$\frac{\partial h_6}{\partial s} = -s(1 - r),$$

$$\frac{\partial h_7}{\partial r} = \frac{1}{2}(1 - s^2),$$

$$\frac{\partial h_7}{\partial s} = -s(1 + r),$$

$$\frac{\partial h_8}{\partial r} = \left(\frac{1}{4}s + \frac{1}{2}r \right) (1 - s),$$

$$\frac{\partial h_8}{\partial s} = (1 - r) \left(\frac{1}{2}s + \frac{1}{4}r \right),$$

$$\frac{\partial h_9}{\partial r} = -r(1 - s),$$

$$\frac{\partial h_9}{\partial s} = -\frac{1}{2}(1 - r^2),$$

$$\frac{\partial h_{10}}{\partial r} = (1 - s) \left(\frac{1}{2}r - \frac{1}{4}s \right),$$

$$\frac{\partial h_{10}}{\partial s} = (1 + r) \left(\frac{1}{2}s - \frac{1}{4}r \right).$$

To ensure monotonic convergence of the solutions obtained by the finite element method to the accurate solution, the shape functions must be selected to satisfy the following conditions.

- The elements should satisfy the conditions of rigid motion and make it possible to model constant strain over the region of a single element.
- The displacements at the edges (the connections) of neighbouring elements should be continuous between the nodes (compatibility of elements).

Satisfaction of the first of those conditions is equivalent, for isoparametric elements, to the satisfaction of the condition $\sum h_i(r, s) = 1$ (h_i - shape functions). It is easy to see that this equation is satisfied by the proposed shape functions.

As regards the second condition (compatibility), it is satisfied (if the element is used in agreement with the scheme of Fig. 3) at the edges 1-8, 8-10 and 10-5 only (Fig. 2), that is at the edges with 3 nodes only. The shape functions for those edges are the same for both types of elements. As regards the edge 1-5, the condition is satisfied at the nodes only. If the second condition is not satisfied, the solutions remain convergent, the convergence being not monotonic, however.

Because the second condition is not satisfied, an additional patch-test was performed by determining the stress in a cylinder subjected to tension and modelled by the element meshes illustrated in Fig. 5.

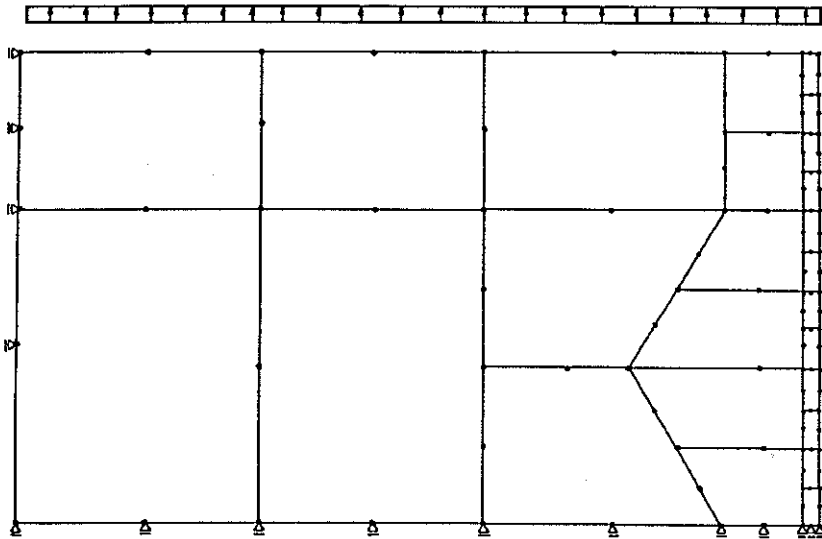


FIG. 5. Element meshes used for testing an element.

The test performed showed accuracy provided all the elements were rectangular. If some of them were degenerate as shown in Fig. 5, the values obtained for the stress would differ from the accurate values by no more than 1.2%. This result is worse than the results obtained with eight-node elements, for which the error was found to be about 0.01%.

The problem of connecting incompatible elements has also been extensively analysed in papers concerned with finite element analysis, [7] and [8], for instance. One of the possible ways of approach is to introduce a penalty function, the aim of which is to minimize the error. This requires, however,

introducing additional unknowns into the set of equations, the solution as a whole thus becoming much more complicated. Taking into account the above fact it was found that the element considered may be used without introducing additional functions, because the error thus committed is admissible in an analysis made for engineering purposes. A problem closely connected with the accuracy is that of integrating the stiffness matrix of an element. Following the directions of [6] and taking into consideration the order of the shape functions used, the integration should be performed according to the 5×3 scheme, that is 5 Gaussian points in the r -direction and 3 Gaussian points in the s -direction. However, after a number of tests which had been made, it was found that the 4×3 scheme is sufficient. This corresponds to the reduced integration of elements which is often used in FEM systems.

4. EXAMPLE OF APPLICATION

As an example of application of the proposed element the state of stress was determined for a specimen with a notch, the dimensions of which are shown in Fig. 6, subjected to tension by a force P . The aim of the analysis

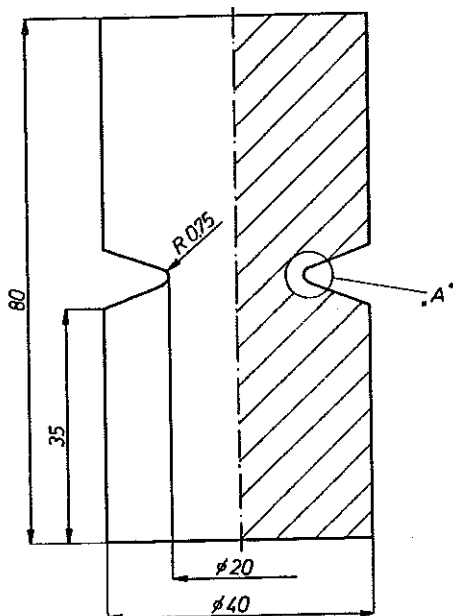


FIG. 6. The specimen with a notch.

was to make sure that the method proposed here for modelling a specimen with a surface layer enables us to obtain some essential information on the reduced stress of the material of the layer.

Two element meshes were used. One of them, which will be referred to as meshes *A*, included elements of the proposed type, which were connected to traditional elements modelling the technological surface layer. With the other mesh, termed *B*, the layer was modelled by membrane type elements [1]. The meshes have not been represented here due to the lack of space, the mesh *A*, for instance, including 132 elements and 491 nodes. A fragment of the mesh "A", at the bottom of the notch, is shown in Figs. 7 to 9.

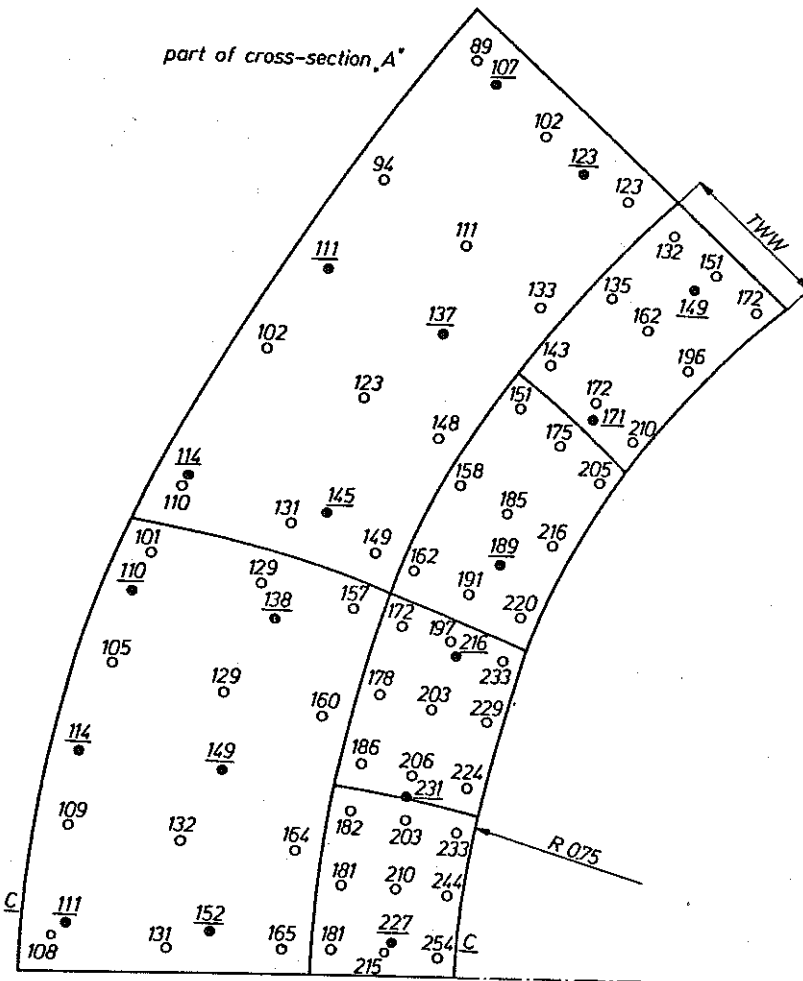


FIG. 7. The stress in the homogeneous specimen under purely elastic strain.

The surface layer was assumed to be 0.2 mm in thickness and the material constants of the core were

$$E = 200000 \text{ MPa}, \quad E^T = 20000 \text{ MPa} \quad (\text{strain-hardening modulus}),$$

$$\nu = 0.3 \quad \text{and} \quad \sigma_e = 400 \text{ MPa}.$$

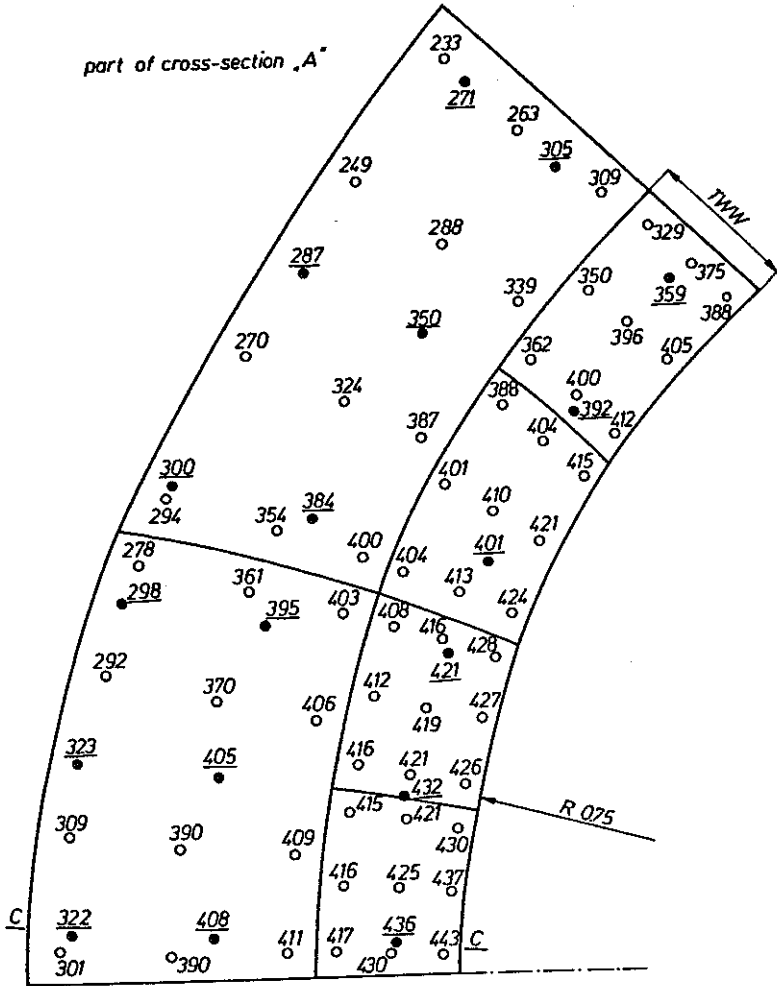


FIG. 8. The stress in the homogeneous specimen under partially plastic strain.

The analysis was made in two cases, which were those of a homogeneous specimen (the material constants in the region of the surface layer being assumed to be the same as in the core), and a specimen with its surface layer characterized by a higher yield point ($\sigma_e = 800 \text{ MPa}$). The material

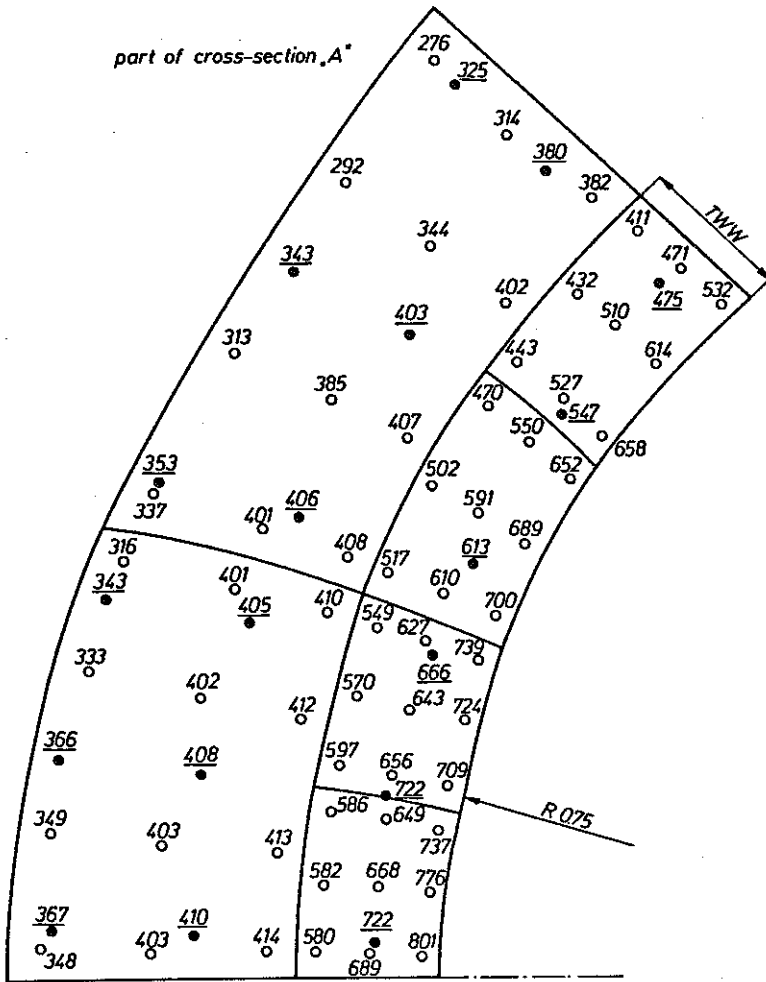


FIG. 9. The stress in a specimen with a surface layer of a higher yield point.

properties were assumed to vary in a jump-like manner. Confrontation of the results obtained for the homogeneous specimen by means of the meshes *A*, elements of the proposed type being located in the region below the surface layer (Figs. 7 to 9), and the mesh *B* in which only eight-node elements are present in this region, enables us to verify, to some extent, the proposed type of elements in regions of high stress gradients.

The results are confronted in several consecutive figures by showing values of the reduced stress (in MPa) obtained for the meshes *A* and *B*. This confrontation has been done for a few elements within the region indicated by a circle (Fig. 6) and located at the bottom of the notch, which is a region of highest stress concentration. The Gaussian points referring to the mesh

A and those referring to the mesh B are marked on a fragment of the meshes A with \circ and \bullet , respectively. The corresponding values of the stress have been put beside those points. The values referring to the meshes B have been underlined for better lucidity. In the case of a homogeneous specimen two values have been assumed for the force P , the first ($P = 31.4 \text{ kN}$) corresponding to a purely elastic state (Fig. 7), and the other ($P = 81.68 \text{ kN}$) – to the case of a small plastic region formed at the bottom of the notch (Fig. 8).

A specimen with a technological surface layer was subjected to tension by a force $P = 98 \text{ kN}$ producing a small plastic region at the bottom, under the layer. The results of the analysis are shown in Fig. 9.

5. INFERENCES

An analysis of Figs. 7, 8 and 9 enables the following conclusions to be drawn. The agreement between the results obtained for either of the two models is the best in the case of elastic strain of a homogeneous specimen. The conclusions drawn from [1] and suggesting that the stress calculated for a layer treated as a membrane (meshes B) is equal to the arithmetic mean of the actual extreme values of the stress in the cross-section of the layer, have been confirmed, which can be seen in the $c - c$ section, for instance. The values of the stress in the zone of the adjacent core to the layer, obtained from the two models, comply fairly well with each other and confirm the agreement between the geometrical model proposed in [1] and the theoretical predictions. Similar conclusions can be drawn by considering the stress field in a homogeneous specimen in a partially plastic state, although the numerical value of the stress is somewhat too high in the zone of the core adjacent to the layer.

In the case of a notch and a layer with a higher yield point (Fig. 9), the values of the stresses obtained from the membrane model approach also the arithmetic mean in the section considered, but the stress gradients are too high, so that the arithmetic mean differs considerably from the maximum value, the membrane model yielding inaccurate results.

The influence of the normal stress component σ_r in the surface layer (neglected in the membrane model) has been taken into account in the values of reduced stress (for the meshes A) which are shown in Figs. 7 to 9. It is worthwhile, however, to add that the value of that stress component is about 100 MPa despite the thickness of the layer being small.

The above conclusions confirm the usefulness of the proposed transitional

elements. In the next stage of the work we expect to introduce the possibility of assuming different values of the material constants for different Gaussian points of the same element. This will make it possible to consider the cases of variable material constants of the surface layer without the necessity of using finer elements for the element mesh.

This work has been carried out within the framework of the research program No 770239203 – Methods for determining the effort of the technological surface layer of machine elements.

REFERENCES

1. Z. HANDZEL-POWIERŻA, S. KUCHARSKI, G. STARZYŃSKI and M. DĄBROWSKI, *Methods for determining stress fields in elements with a technological surface layer in an elastic-plastic state of strain* [in Polish], Zesz. Naukowe PW, Warszawa 1990.
2. Z. HANDZEL-POWIERŻA and S. KUCHARSKI, *Determination of stresses in a structure with a technological surface layer by the method of finite elements* [in Polish] Engng. Trans., **38**, 3–4, 635–647, 1990.
3. K. KOMVOPOULOS, *Finite element analysis of a layered elastic solid in normal contact with a rigid surface*, ASME, J. Tribology, **110**, 477–485, 1988.
4. SATOSHI ODA and KOUTSU MIAYACHIKA, *Residual stress calculation of case hardened thin-rimmed spur gears with various standard pressure angles*, The Third International Conference on Residual Stresses, ICRS-3, Tokushima, Japan 1991.
5. P. MONTMITONNET, M.L. EDLINGER and E. FELDER, *Finite element analysis of elastoplastic indentation. Part II. Application to hard coatings*, J. Tribology, **115**, 15–19, 1993.
6. K.J. BATHE, *Finite-Elemente-Methoden*, Springer Verlag 1990.
7. P. TSAI and W.H. CHEN, *The combination of different type elements using a Lagrangian multiplier technique for static and dynamic structural analysis*, Computers and Structures, **21**, 493–500, 1985.
8. G.F. CAREY, A. KABAILA and M. UTKU, *On penalty methods for interelement constraints*, Comp. Meth. Appl. Mech, Engng., **30**, 151–171, 1982.

POLISH ACADEMY OF SCIENCES
INSTITUTE OF FUNDAMENTAL TECHNOLOGICAL RESEARCH.

Received July 2, 1993.